Oral Oncology 168 (2025) 107583

Contents lists available at ScienceDirect

Oral Oncology

journal homepage: www.elsevier.com/locate/oraloncology

The interplay of hypoxia, inflammation, and microbiota as indicators of malignant transformation in oral potentially malignant disorders

Cristina Gurizzan [a,1], Armando G. Licata [b,1], Luigi Lorini [a], Cesare Piazza [c], Davide Mattavelli [c,d], Alberto Paderno [e,f], Simonetta Battocchio [g], Laura Ardighieri [g], Anna Bozzola [g], Carlo Resteghini [a,e], Chiara Magri [h], Chiara Romani [i], Deborah Lenoci [b], Marta Lucchetta [b], Mara S. Serafini [b], Loris De Cecco [b,1,*], Paolo Bossi [a,e,1,**]

[a] Medical Oncology and Hematology Unit, IRCCS Humanitas Research Hospital, Rozzano, Milan, Italy
[b] Integrated Biology of Rare Tumors, Department of Experimental Oncology, Fondazione IRCCS Istituto Nazionale dei Tumori, Milan, Italy
[c] Unit of Otorhinolaryngology - Head and Neck Surgery, ASST Spedali Civili di Brescia, Brescia, Italy
[d] Department of Medical and Surgical Specialties, Radiological Sciences, and Public Health, University of Brescia, Brescia, Italy
[e] Department of Biomedical Sciences, Humanitas University, Milan, Italy
[f] Otorhinolaryngology Unit IRCCS Humanitas Research Hospital, Rozzano, Milan, Italy
[g] Unit of Pathology, ASST Spedali Civili di Brescia, Brescia, Italy
[h] Medical Oncology Unit, Department of Medical and Surgical Specialties, Radiological Sciences and Public Health, University of Brescia, ASST Spedali Civili, Brescia, Italy
[i] Angelo Nocivelli Institute of Molecular Medicine, University of Brescia and ASST Spedali Civili di Brescia, Brescia, Italy

ARTICLE INFO

Keywords:
Oral potentially malignant disorders
Malignant transformation
Hypoxia
Oral microbiome

ABSTRACT

Oral Potentially Malignant Disorders (OPMDs), such as leukoplakia, erythroplakia, proliferative verrucous leukoplakia, and oral submucous fibrosis, carry a risk of malignant transformation, with reported rates ranging from 2.6 % to 7.9 %. Higher risks are observed in specific subtypes, such as erythroplakia and proliferative verrucous leukoplakia. Although clinical factors like lesion size, dysplasia, and patient demographics have been studied, none have consistently proven reliable for predicting malignancy. This study conducted a retrospective review of OPMD patients treated at the University of Brescia from 1996 to 2019, including various dysplasia grades and extensive clinical data. Gene expression profiling was performed on these samples to explore molecular stratification based on a six-subtype classification developed for Head and Neck Squamous Cell Carcinoma (HNSCC). Additionally, intratumor microbiota content was analyzed to assess its association with OPMD transformation risk. The findings highlighted the aggressive nature of the Cl3-Hypoxia molecular subtype, with a median malignant transformation time of 30.1 months. Considering the role of hypoxia in modulating tumor-associated inflammatory cell functions, we also assessed two inflammatory gene signatures, demonstrating their significant association with OPMDs and correlating with tissue-resident microbiota. This study provides compelling evidence of microbial-host interactions in the malignant transformation of OPMDs, with specific molecular features, particularly hypoxia-related pathways, linked to increased malignancy risk. These results suggest potential biomarkers for prognosis and offer therapeutic strategies targeting the tumor microenvironment and microbiota to mitigate malignant progression in high-risk OPMD patients.

Introduction

The term Oral Potentially Malignant Disorders (OPMD) was first delineated in 2007 by the WHO Collaborating Centre for Oral Cancer to encompass a diverse spectrum of pathological conditions affecting the oral cavity, sharing a common characteristic of potential malignant

* Corresponding author at: Integrated Biology of Rare Tumors, Department of Experimental Oncology, Fondazione IRCCS Istituto Nazionale dei Tumori, Via Amadeo, 42, 20133 Milano, MI, Italy.
** Corresponding author at: IRCCS Humanitas Research Hospital, via Manzoni 56, 20089 Rozzano, Milan, Italy
E-mail addresses: Loris.DeCecco@istitutotumori.mi.it (L. De Cecco), paolo.bossi@hunimed.eu (P. Bossi).
[1] these authors equally contributed to the paper.

https://doi.org/10.1016/j.oraloncology.2025.107583
Received 16 May 2025; Received in revised form 27 July 2025; Accepted 31 July 2025
Available online 8 August 2025

transformation [1]. Oral leukoplakia and erythroplakia, proliferative verrucous leukoplakia, oral submucous fibrosis, and oral lichen planus/lichenoid lesions are the most commonly disorders [2]. A *meta*-analysis incorporating 22 published studies estimated a global prevalence of OPMDs at 4.47 % (95 % CI = 2.43–7.08), with higher prevalence rates observed in males (59.99 %; 95 % CI = 41.27–77.30) and Asian populations (10.54 %; 95 % CI = 4.60–18.55) [3,4]. The malignant transformation rates across various subtypes of OPMD range from 2.6 % to 7.9 % [5,6].

To date, several clinical factors have been investigated as potential predictors of malignant progression, including gender, age, oral cavity subsite, lesion size, and presence of dysplasia. However, none have proven consistently reliable in identifying disorders at higher risk of transformation [7]. Iocca et al., through a systematic review and *meta*-analysis reported significantly higher malignant transformation rates for oral erythroplakia (33.1 %; 99 % CI 13.6 %-56.1 %) and proliferative verrucous leukoplakia (49.5 %; 99 % CI 26.7 %-72.4 %) [8]. Recently, a clinical nomogram utilizing age, oral cavity subsite, disorder subtype, dysplasia presence, and medical history of other cancers has been proposed to predict the risk of malignant transformation [5]. Furthermore, considerable attention has been directed towards molecular biomarkers, with loss of heterozygosity (LOH) emerging as a promising indicator for predicting progression to oral cancer. Initially identified in 1996 [9], LOH at specific loci encoding tumor suppressor genes (e.g., 3p14 and/or 9p21) has been associated with a 3-year risk of developing oral cancer of approximately 35 % [10].

Enhancing the prognosis of OPMD patients necessitates a deeper understanding of the biological mechanisms underlying malignant transformation. Recent studies investigating tumor mutational burden (TMB), TP53 mutations, and specific mRNA transcripts have underscored their potential roles in assessing the risk of progression to oral cancer in large cohorts of oral premalignant lesions [11].

In a previous study, we demonstrated that our six molecular cluster subtyping in Head and Neck Squamous Cell Carcinoma (HNSCC) are also applicable to OPMD highlighting their biological properties [12]. In this investigation, gene expression profiles of 86 OPMD cases were analyzed, revealing that patients exhibiting Mesenchymal, Hypoxia, and Classical signatures face a heightened risk of malignant progression.

Recent studies have emphasized the significant role of gut microbiome dysbiosis in colorectal cancer, indicating that integrating microbiome data may offer synergistic diagnostic advantages [13]. Other research has also revealed the presence of metabolically active, immune-responsive, and cancer type-specific bacterial, viral, and fungal communities within tumor tissues [14–16]. These discoveries have contributed to their inclusion in the updated cancer hallmarks [17], highlighting their relevance across various cancer types.

However, our understanding of the oral microbiota—the second most diverse microbial community in the human body—and its impact on oral potentially malignant disorders (OPMDs) remains limited.

The principal aim of our present study is to validate the performance of our molecular stratification in an independent series of dysplastic OPMD cases. In this way, our work seeks to establish a robust framework for prognostic assessment and therapeutic stratification in OPMD. Our secondary objective is to investigate the relationship between molecular clusters and the tissue microbiota within these lesions.

Material and methods

Study design and patients' cohort

Clinical data of OPMDs patients treated with complete excision at the Department of Otolaryngology-Head and Neck Surgery of the University of Brescia, Italy, between March 1996 and November 2019 were retrieved and reviewed. Inclusion criteria for the present study were: (a) histological diagnosis of OPMD, treated with curative intent surgery (i.e., resection of the whole lesion in healthy margins) and showing any grade of dysplasia at pathological exam, (b) histological information regarding grade of dysplasia and margins of resection, (c) available archival histological material for gene expression analysis, and (d) availability of follow-up information regarding local recurrence either as dysplasia or carcinoma.

Patients with diagnosis of synchronous head and neck squamous cell carcinoma and previous history of oral cavity cancer within 2 years were excluded.

A written informed consent was obtained from all patients and data management was conducted in accordance with the Declaration of Helsinki; the study was approved by the local ethics committee of Brescia (study number NP4713).

Gene expression profiling

RNA was extracted from 8 mm-thick FFPE slices using the miRNeasy kit (Qiagen) and following manufacturer's instructions. RNA concentration was assessed with Qubit Fluorometer (ThermoFisher) while quality was evaluated using 4150 TapeStation System RNA ScreenTape (Agilent). Sequencing libraries were constructed from 100 ng of total RNA using the QuantSeq 3′ mRNA-Seq Library Prep Kit FWD for Illumina (Lexogen), following manufacturer's instructions and modifications for FFPE material. After quality check on D1000 ScreenTape (Agilent), libraries were equimolarly pooled and sequenced on a NextSeq 500 (Illumina) to an average depth of 7 × 106 single-end reads.

Bioinformatics and statistical analyses

FASTQ files were processed using the QuantSeq 3′ mRNA-seq pipeline implemented on the Bluebee genomic platform (Bluebee, Lexogen). The gene count matrix was imported into R, filtered, and normalized. We then applied our model [18] to stratify the gene expression profiles into molecular subtypes. Briefly, the Prediction Analysis for Microarrays (PAM) algorithm [19] was utilized to apply the six clusters to our dataset. PAM, a widely-used method for classifying high-dimensional data, operates through a nearest shrunken centroid approach. This method involves creating a classification rule based on the scaled distances between expression profiles of new samples and class centroids. Specifically, PAM shrinks the centroids of classes towards the overall means while incorporating a mechanism for variable selection. Two inflammation signatures were selected from literature [2021]. The list of genes and coefficients were retrieved from the papers; the signature from Jing et al. includes 5 inflammatory-related genes, while Han et al contains 14 genes. Calculations to impute the signature scores were made using hacksig R package [22]. The receiver operating characteristic (ROC) curve was used to assess the accuracy of the inflammation signatures in discriminating Cl3-Hypoxia compared to the other. ROC, the area under the curve (AUC), and confidence intervals were calculated and visualized using pROC R package [23].

Class prediction analysis was done using the Diagonal Linear Discriminant Analysis (DLDA) and we then used leave-one-out cross-validation (LOOCV) to estimate the extent to which Cl3 cases could be discerned from the cases assigned to the other clusters. Statistical analyses were done using the BRBArrayTools package (version 6.3.3_beta1) developed at the Biometrics Research Branch of the National Cancer Institute (http://linus.nci.nih.gov/BRB-ArrayTools.html). For validation purposes, eighty-six oral premalignant cases enrolled in a randomized chemoprevention trial at University of Texas MD Anderson Cancer Center (Houston, TX 77030, USA) and profiled by microarray gene expression were retrieved from GEO (ID: GSE26549) to apply the DLDA model.

Kaplan-Meier survival analyses for both the six molecular subtypes and the four prognostic signatures were conducted using the R package survival. The ggplot2 package [24] was employed to visually represent the survival curves, with time to transformation as the clinical endpoint defined as the time (months) from histological diagnosis to cancer

development in the same area of OPMD. Bioinformatic analyses were performed using R software version 4.3.0.

Metagenomic profiling of bacterial reads from gene expression data

To investigate the microbial composition within gene expression data, a metagenomic pipeline was implemented. Initially, raw FASTQ files from bulk RNA-seq underwent processing to extract bacterial reads, involving adapter removal and Unique Molecular Identifier (UMI) extraction using Cutadapt and UMI-tools, respectively. Subsequently, the KneadData decontamination pipeline was employed to eliminate host sequences, specifically removing reads aligned to the human reference genome and transcriptome. The resulting decontaminated FASTQs underwent taxonomic classification via Kraken2, utilizing a bacterial database built following kraken's manual. Kraken2 provided taxonomic assignments, classifying bacterial sequences and generating a read count report for each sample. These reports were then merged and imported into R software, alongside data from gene signature classification analysis. Microbial richness and composition were analyzed using the Phyloseq [25] package (version 1.42.0). The imported data underwent preprocessing, involving normalization through standardizing abundances to the median sequencing depth and feature filtering using a Coefficient of Variation cutoff of 3. The feature table was subsequently employed to evaluate ecological diversity (alpha and beta), and DeSeq2 [26] was applied to identify group-specific differentially abundant features.

Metagenome functional analysis

The microbial transcriptome was investigated using bacterial sequences identified by kraken2. The bacterial reads generated from kraken2 were subjected to translation research against the Swiss-Prot protein database using the Diamond aligner [27]. Diamond, a sequence aligner designed for protein and translated DNA searches, was employed to identify the protein profile of our samples. Subsequently, these profiles were clustered into pathways or proteins by retrieving protein annotations through Uniprot.ws. The abundances of these proteins were then inferred. Following this, a differential abundance analysis was conducted using the LinDA R package [28]. The analysis incorporated the Benjamini-Hochberg procedure within the LinDA package to adjust p-values. Proteins with Log2FoldChange > 1 and adjusted p-value < 0.05 were accepted as differentially expressed proteins. The protein interaction network was created using STRING and visualized with Cytoscape v3.10 [29].

Results

Patients' characteristics

A total of 106 consecutive OPMDs patients were retrieved. Of these, 66 fulfilled the eligibility criteria and were suitable for gene expression analysis after RNA extraction and quality checks. As depicted in Table 1, a slight majority were male (53 %), with a median age of 65 years (range 32–94), data regarding smoking habits were available only for 28 patients, and among them 14 (21.2 %) were current smokers at the time of database completion. Eleven patients (16.7 %) had a previous diagnosis of oral cavity cancer carcinoma (OCC). Regarding OPMDs grade of dysplasia, 28 patients (42.2 %) presented with grade 1 (SIN1) dysplasia, 23 (34.9 %) with grade 2 (SIN2), 8 (12.1 %) with grade 3 (SIN3), while 7 patients had a diagnosis of carcinoma in situ (CIS). With a median follow-up of 53 months (range 14–234), 22 patients (33.3 %) experienced an OPMD recurrence, and 15 patients (22.7 %) had a histologically proven malignant transformation to OCC, with a median time to transformation of 30 months (range 3–195).

Table 1
Patients and disease characteristics.

Patients number (66)	Characteristics	Number (%)	Number (%) Cluster 3 (10 patients)
Gender	Female	31 (47)	6 (60)
	Male	35 (53)	4 (40)
Age at diagnosis		Median 65 (range 32–94)	Median 69.5 (range 64–94)
Smoking history	Current smoker	14 (21.2)	1 (10)
	Former smoker	4 (6.1)	1 (10)
	Never smoker	10 (15.1)	1 (10)
	Not available	38 (57.6)	7 (70)
History of OCC	Yes	11 (16.7)	4 (40)
	No	55 (83.3)	6 (60)
Grade of dysplasia	SIN1	28 (42.4)	1 (10)
	SIN2	23 (34.9)	5 (50)
	SIN3	8 (12.1)	3 (30)
	CIS	7 (10.6)	1 (10)
OPMD recurrence	Yes	22 (33.3)	7 (70)
	No	44 (66.7)	3 (30)
Malignant transformation	Yes	15 (22.7)	7 (70)
	No	51 (77.3)	3 (30)
Median follow-up		53 months (range 14–234)	44 months (range 15–125)

Six molecular subtype stratification

Six distinct subtypes delineating the heterogeneous molecular profiles implicated in tumor progression were identified within HNSCC. These subtypes, characterized by their distinct biological features and dysregulated signaling pathways, were categorized as follows: Cl1-HPV, Cl2-Mesenchymal, Cl3-Hypoxia, Cl4-Defense Response, Cl5-Classical, and Cl6-Immunoreactive. The PAM algorithm was employed to extend our classification framework to OPMD. The application of PAM revealed that none of the cases fell into Cl1-HPV, 5 cases (8 %) were classified as Cl2-Mesenchymal, 10 cases (15 %) exhibited characteristics of Cl3-Hypoxia, 18 cases (27 %) were identified as Cl4-Defense Response, 6 cases (9 %) represented Cl5-Classical, and 27 cases (41 %) were categorized under Cl6-Immunoreactive. The subtype stratification confirms significant difference in outcome having time to transformation as clinical endpoint and median time is equal to 175.9 months for Cl2-Mesenchymal, 30.1 months for Cl3-Hypoxia, not-reached for Cl4-Defense Response, 142.8 months for Cl5-Classical, and not reached for Cl6-Immune Reactive (Fig. 1).

Characteristics of patients belonging to different clusters are depicted in Table 2.

We then decided to compare the characteristics of the hypoxic cluster against the group of all other clusters (Table 3). Hypoxia cluster showed a higher risk of malignant transformation ($p < 0.0001$) and a greater risk of OPMD recurrence (p 0.021).

The association between our molecular stratificatiand the various oral potentially malignant disorders, including leukoplakia, erythroplakia, and others, was systematically investigated. A focused analysis on leukoplakia, the most prevalent entity in our cohort, confirmed a statistically significant difference in clinical outcomes. Specifically, the Cl3 molecular subtype exhibited a median time to malignant transformation of 30.1 months, whereas this endpoint was not reached for the remaining clusters. This corresponded to a hazard ratio (HR) of 7.01 (95 % CI: 1.25–39.3), $p = 0.011$ (Supplementary Fig. 1).

Univariable Cox proportional hazards models, incorporating a binary stratification (Cl3 vs. other clusters) and OPMD clinical entities (leukoplakia vs. erythroplakia and others), demonstrated that the Cl3 subtype is significantly associated with increased risk of malignant transformation. Furthermore, multivariable Cox models confirmed that Cl3 represents an independent prognostic factor (Supplementary Table 1).

To enable predictive classification of the Cl3 subtype within our

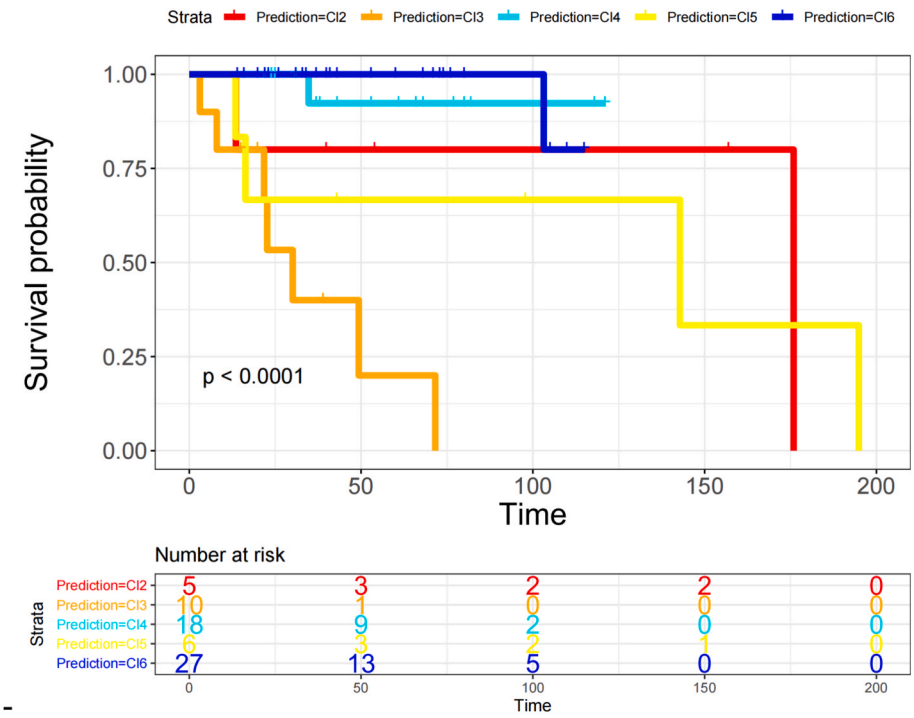

Fig. 1. Six molecular subtypes. The six molecular HNSCC subtype classifications were applied to the OPMDs. including 66 patients. The six clusters evidenced differences in terms of probability of time to transformation (p = 2.69E-07, log-rank test). The 5-year proportion of patients not experiencing malignant transformation is 0.8 for Cl2-Mesenchymal, 0.2 for Cl3-Hypoxia, 0.923 for Cl4-Defense Response, 0.667 for Cl5-Classical, and 1 for Cl6-Imunereactive. Cl2- Mesenchymal, red; Cl4-Defense Response, blue; Cl3-Hypoxia, orange; Cl5-Classical, yellow; Cl6,-Imunereactive light blue. (For interpretation of the references to colour in this figure legend, the reader is referred to the web version of this article.)

Table 2
Molecular subtype stratification.

Patients number (66)	Characteristics	Cluster 2 (5 pts)	Cluster 3 (10 pts)	Cluster 4 (18 pts)	Cluster 5 (6 pts)	Cluster 6 (27 pts)
Gender	Female	3 (60)	6 (60)	9 (50)	4 (67)	9 (33)
	Male	2 (40)	4 (40)	9 (50)	2 (33)	18 (67)
Age at diagnosis	Median	47	69.5	62.5	70.5	63
		(range 36–70)	(range 64–94)	(range 32–88)	(range 60–78)	(range 32–80)
Smoking history	Current smoker	0	1 (10)	6 (32)	0	7 (26)
	Former smoker	0	1 (10)	0	1 (17)	2 (7)
	Never smoker	1 (20)	1 (10)	2 (12)	2 (33)	4 (15)
	Not available	4 (80)	7 (70)	10 (56)	3 (50)	14 (52)
History of OCC	Yes	1 (20)	4 (40)	1 (6)	1 (17)	4 (15)
	No	4 (80)	6 (60)	17 (94)	5 (83)	23 (85)
Grade of dysplasia	SIN1	3 (60)	1 (10)	7 (28)	1 (17)	16 (59)
	SIN2	0	5 (50)	9 (50)	3 (50)	6 (22)
	SIN3	1 (20)	3 (30)	1 (6)	1 (17)	2 (7)
	CIS	1 (20)	1 (10)	1 (6)	1 (17)	3 (12)
OPMD recurrence	Yes	2 (40)	7 (70)	4 (22)	4 (67)	5 (19)
	No	3 (60)	3 (30)	14 (78)	2 (33)	22 (81)
Malignant transformation	Yes	2 (40)	7 (70)	1 (6)	4 (67)	1 (4)
	No	3 (60)	3 (30)	17 (94)	2 (33)	26 (96)
Median follow-up	Median months	54	44	57	94.5	43
		(range 39–173)	(range 15–125)	(range 22–121)	(range 18–234)	(range 14–119)

OPMD cohort, a gene expression–based classifier was developed. Using LOOCV with a Diagonal Linear Discriminant Analysis (DLDA) approach, a 110-gene signature was identified. The classification rule is defined by a weighted score, calculated as the sum of the products of gene expression levels (xi) and their corresponding weights (wi), according to the formula: $\sum i(wi \times xi)$. Higher scores indicate a greater probability of classification as Cl3. The full list of genes and their associated coefficients is provided in Supplementary Table 2.

This DLDA-based classifier was applied to the external and independent dataset GSE26549 for validation. The Cl3 classification was again associated with significantly poorer outcomes, with a median time to transformation of 27.24 months, compared to an unreached median for the other clusters. The corresponding hazard ratio was 3.15 (95 % CI: 1.53–6.49), p = 0.0011 (Supplementary Fig. 2).

Two signatures identified from genes related to the inflammatory response, which enable risk stratification for predicting clinical outcomes in HNSCC, were tested in OPMD (Fig. 2). Following the methods from the original studies, a high score was associated with increased risk. Patients predicted to belong to the Cl3-Hypoxia cluster, as well as other clusters, were assessed for their signature scores. Cl3-Hypoxia cases exhibited significantly higher scores for the Jing et al. signature (p = 0.023, Fig. 2A), with an AUC of 0.729, 95 % CI (0.5529–0.9043)

Table 3
Cl3-Hypoxia cluster versus different clusters.

	Characteristics	Cluster 3 (10 patients)	Cluster 2–4-5–6 (56 patients)	p
Gender	Female	6 (60)	25 (45)	0.548
	Male	4 (40)	32 (55)	
Smoking history	Current	1 (10)	13 (23)	0.677
	smoker	1 (10)	3 (5)	
	Former smoker	1 (10)	9 (16)	
	Never smoker	7 (70)	31(66)	
	Not available			
History of OCC	Yes	4 (40)	12 (21)	0.309
	No	6 (60)	49 (79)	
Grade of dysplasia	SIN1	1 (10)	27 (48)	0.078
	SIN2	5 (50)	18 (32)	
	SIN3	3 (30)	5 (9)	
	CIS	1 (10)	6 (11)	
OPMD recurrence	Yes	7 (70)	15 (27)	**0.021**
	No	3 (30)	41 (73)	
Malignant transformation	Yes	7 (70)	8 (14)	**> 0.001**
	No	3 (30)	48 (86)	

(Fig. 2B). Similarly, Cl3-Hypoxia cases showed a significant association with the Han et al. signature ($p = 0.033$, Fig. 2C), achieving an AUC of 0.714, 95 % CI (0.5516–0.877) (Fig. 2D).

Microbial Dynamics in hypoxic gene expression profiles

In exploring the dynamic relationship between the microbiome and the host's gene expression profile, we extracted bacterial reads and conducted alignment against the NCBI bacterial database. The resultant taxonomic alignment yielded a matrix of bacterial read counts (Minimum = 2,295, 1st Quartile = 27,684, Median = 49,281, 3rd Quartile = 91,928, Maximum = 233,995). Subsequent analysis involved comparing the microbial profiles between samples with Cl3-Hypoxia (10 samples) and those belonging to different clusters (56 samples) such as Cl1-HPV, Cl2-Mesenchymal, Cl4-Defense Response, Cl5-Classical, and Cl6-Immunoreactive (Fig. 3). The relative abundance of genera with an abundance > 0.3 % is depicted in (Fig. 3A), indicating a consistent microbial composition between Cl3-Hypoxia and those with the others. Noteworthy findings include Fusobacterium (11.30 %) and Leptotrichia (10.68 %) as the dominant oral bacterial genera in patients predicted as Cl3-Hypoxia, alongside Enterobacter (9.11 %) and Klebsiella (6.28 %). Conversely, in patients belonging to the other clusters, Halomonas (9.07 %) and Leptotrichia (8.6 %) emerged as the predominant genera. The oral microbiome diversity of the 10 Cl3-Hypoxia patients showed a lower diversity than the other clusters (Fig. 3B). Alpha-diversity, as measured by Observed features, exhibited no significant difference between Cl3-Hypoxia and other clusters ($p > 0.05$). However, the Shannon and inverse Simpson indexes indicated lower abundance and diversity in Cl3-Hypoxia patients compared to the other group ($p = 0.013$) and ($p = 0.02$), respectively. Taxonomy-based principal coordinate analysis (PCoA) revealed no significant differences in beta-diversity among the various clusters ($p > 0.05$). (Fig. 3C). The DESeq2 analysis of the microbiome revealed significant differential abundance in hypoxia conditions for 11 bacterial species (Fig. 3D). Remarkably, species within the *Fusobacterium* and *Pasteurella* genera, such as *Fusobacterium nucleatum* and *Pasteurella multocida*, exhibited consistent upregulation, with log2 fold changes ranging from 2.47 to 3.32 and a −log10(adj.p-value) > 2. Suggesting a substantial impact of hypoxia on the composition of the microbial community.

Metaproteomic analysis reveals differential microbial activity in hypoxic patients

The bacterial reads identified as microbial were subsequently subjected to translated alignment to investigate functional disparities in the microbiome among patients categorized based on their gene expression profiles as either "hypoxic" or "other" (Fig. 4). As expected, the ratios between microbial reads and aligned proteins exhibited inconsistency, suggesting that numerous translated reads corresponded to proteins absent from the Swiss-Prot database (Fig. 4A). In total, 2003 proteins were identified with comprehensive functional and taxonomic annotations. Then we conducted a comparative analysis of protein profiles across our samples to detect any significant distinctions in our dataset (Fig. 4B). Overall, the protein profiles displayed a degree of uniformity, with no noteworthy differences in proteomic correlation, except for a subset of samples belonging to the hypoxic group, as depicted in the dendrogram (Fig. 4B). The LinDA algorithm was utilized to pinpoint differentially abundant bacterial proteins in the hypoxic group (Fig. 4C). This analysis highlighted Q8RIH3 as a significant protein with an adjusted p-value < 0.05 and a Log2FoldChange > 1. Further investigation into the function of Q8RIH3 revealed its derivation from the rpsE gene within Fusobacterium nucleatum's genome, where, in conjunction with other genes, it plays an important role in translational accuracy, as demonstrated in the network (Fig. 4D). Taken together, these results demonstrate that within the hypoxic group, Fusobacterium nucleatum was present and active, as evidenced by the upregulation of the rpsE gene involved in protein transcription, highlighting the potential significance of this microbial activity in hypoxic conditions.

Discussion and conclusions

Defining the subgroup of OPMDs patients' carrying a higher risk of malignant transformation represent one of the main unmet clinical needs in the management OPMDs.

So far, different clinical factors have been proposed as predictors of cancer development, however their role is not well established and only few of them has been recognized as reliable, including history of previous HN cancer, female gender and smoking [7].

Indeed, a huge effort has been made to move to a mechanistic biomolecular signature capable of predict the risk of malignant transformation.

Among the existing biomolecular signature, loss of heterozygosity at specific loci codifying for tumor suppressors genes has proved to carry a higher risk of malignant transformation. However, in the EPOC trial the molecular selection of OPMD patients' candidates to erlotinib through LOH failed in improving oral cancer-free survival [30].

Foy and colleagues [31] moved a step forward by identifying two distinct gene expression subtypes of OPMDs, namely immunological and classical, that were validated in three independent datasets. The immunological subtype was characterized by enrichment of immune pathways, especially lymphocyte-related ones, including PD-1 signaling and CTLA-4 pathway. On the other hand, the classical subtype showed enrichment of pathways involved in xenobiotic metabolism as well as EGFR signaling.

Also, through an in-depth immunological profiling, Hanna and colleagues [32] demonstrated an abundance in CD8+ T cells and T reg, together with PD-L1 overexpression, in high-risk proliferative leukoplakia when compared with the more common localized leukoplakia.

To our knowledge, no other biomolecular signatures have been proposed in the context of OPMDs, and the role of salivary biomarkers in this regard remains to be clarified.

Six distinct subtypes within HNSCC were identified by our team using bioinformatics topological decomposition methods [18]. The process involved transforming the gene expression data from tumor tissues into a composite of two components: a normal-like component reflecting healthy tissue characteristics, and a disease-like component measuring deviations from this normal state. To achieve this, we utilized the Disease-Specific Genomic Analysis (DSGA) tool [33], which employs a data structure decomposition approach to highlight the pathological component within gene expression data. This method simplifies the expression data by separating it into disease-like and normal-like

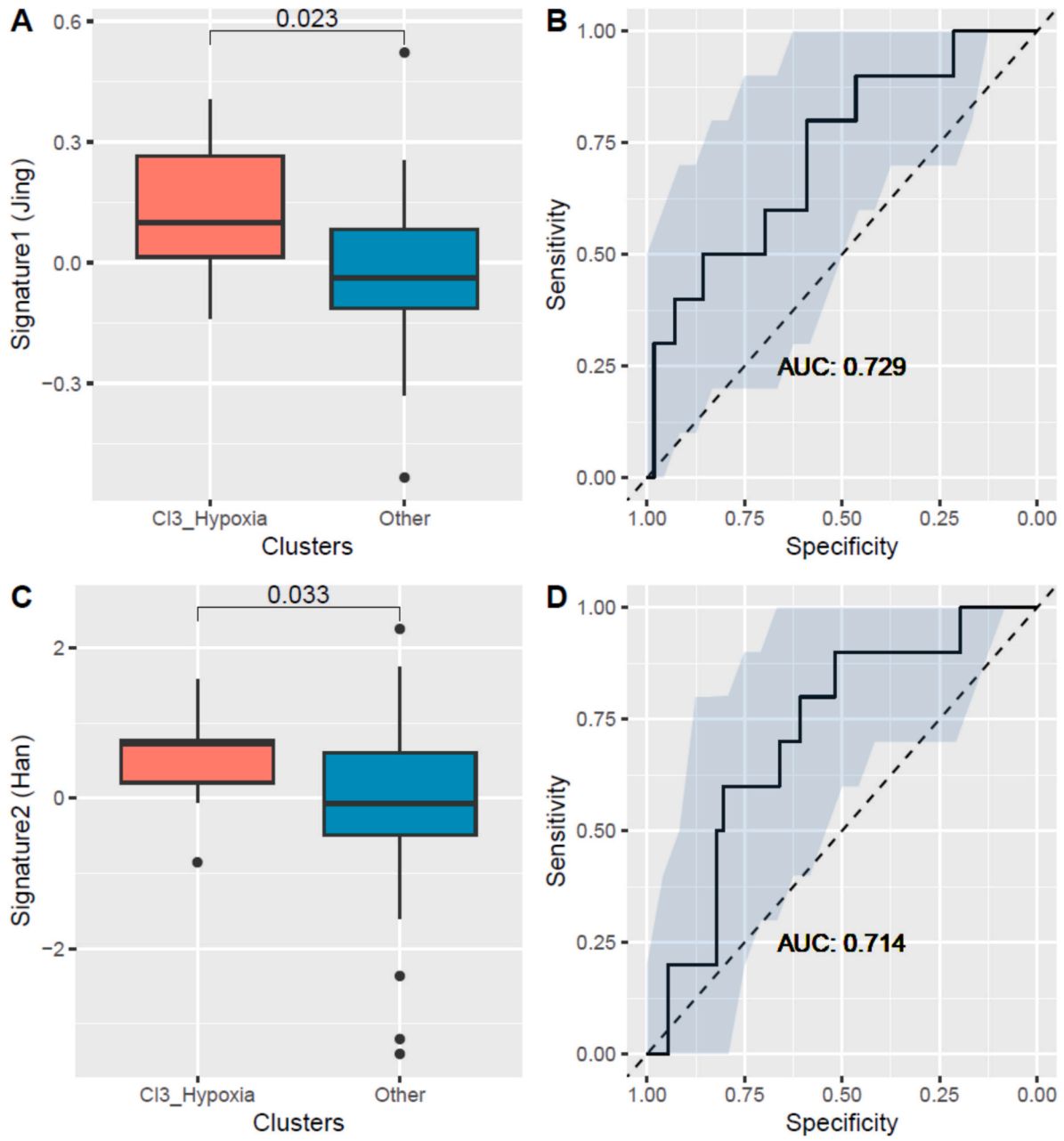

Fig. 2. Inflammation signatures. (A) Box plot of scores for Jing et al signature divided in Cl3-Hypoxia (red, n = 10) and other clusters (blue, n = 56); (B) ROC and AUC for Jing et al; (C) Box plot for Han's et al signature divided in Cl3-Hypoxia (red, n = 10) and other clusters (blue, n = 56); (D) ROC and AUC for Han et al. Gray shadow represent 95 % CI. (For interpretation of the references to colour in this figure legend, the reader is referred to the web version of this article.)

components for each gene, thereby constructing a model of the healthy state based on expression data from normal tissues.

By decomposing each tumor tissue into these two components—normal and disease—we assessed the extent to which tumors deviate from the normal state. This disease component was instrumental in identifying our six molecular subtypes of HNSCC. Notably, Cl6-Immunoreactive and Cl4-Defense Response subtypes exhibited features more akin to the normal state compared to the Cl3-Hypoxia subtype.

Given the unique nature of our approach in quantifying the distance from the normal state, we further investigated the applicability of our HNSCC subtype classification to OPMD datasets. We already conducted a detailed analysis of molecular pathways using a publicly available dataset of oral potentially malignant lesions profiled by gene expression profiles. Our objective was to determine whether and to what extent the molecular profiles typical of HNSCC are also present in premalignant lesions. The majority of cases were stratified as Cl6-Imunereactive and Cl4-Defense Response (60.4 %) and Cl3-Hypoxia represented the one with the worst prognosis, with a 5-year oral cancer-free survival of 30.7 % [12]. These findings were corroborated in our independent cohort, where a predominant classification was observed predominantly in Cl6-Immunoreactive and Cl4-Defense Response subtypes (68 %). Specifically, the Cl6-Immunoreactive subtype exhibited heightened activation of immune-related pathways, such as IFN-I, and our recent studies have indicated that patients categorized within this molecular subgroup derive therapeutic benefits from immunotherapy [34]. Additionally, the Cl6-Immunoreactive cluster demonstrated a positive correlation with favorable prognosis. Conversely, the Cl3-Hypoxia subtype was associated with the poorest outcomes. This subtype holds clinical relevance, especially in the context of HNSCC patients treated with EGFR inhibitors

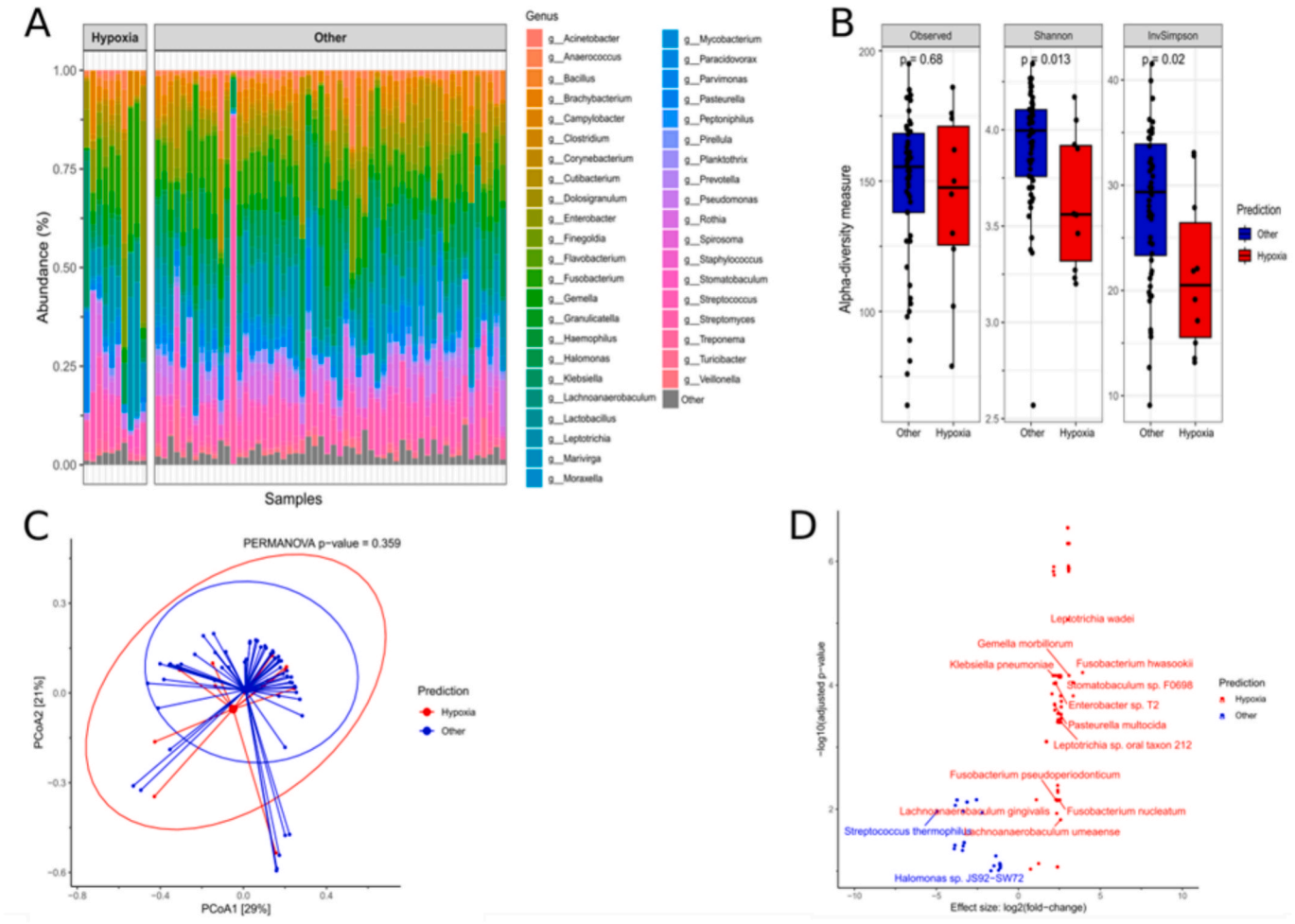

Fig. 3. Microbial Community Analysis of Bacterial Reads (A) Relative abundance distributions at the genus level in samples obtained from patients classified as Cl3-Hypoxia subtype and other subtypes. (B) Alpha-diversity measures (Observed features, Shannon index, and Inverse Simpson) among samples with different gene profile predictions, with statistical analysis performed using the Mann Whitney *U* test. (C) Principal Coordinates Analysis (PCoA) of Bray-Curtis distance on all samples at the species level. The PERMANOVA test was employed to identify independent effects of gene expression profiles on the microbial community (Bray-Curtis distance, 999 permutations). (D) Volcano plot depicting differentially abundant features (adjusted p-value < 0.05, adjustment method "BH") identified using DeSEq2, with emphasis on features taxonomically classified at the species level.

[35–37]. Although the prognostic role of the hypoxia cluster seems uncontroversial even in the OPMDs setting, the reasons behind this evidence remain to be explained. Intratumoral hypoxia is commonly observed in locally advanced cases of HNSCC and is known to contribute to resistance against both radiation therapy and chemotherapy, thereby worsening patient [38]. Hypoxia and inflammation are closely interconnected, with hypoxic conditions not only affecting tumor cells but also influencing the surrounding microenvironment, including cells involved in inflammatory responses. In our study, we tested two gene signatures associated with inflammation, originally developed for HNSCC, and confirmed their relevance in OPMD. Our findings underscore the critical biological interplay between hypoxia and inflammation in driving malignant transformation.

In a review illustrating the role of hypoxia in oral carcinogenesis, Kujan and colleagues [39] showed how dysregulation of hypoxia proteins is an early event in oral carcinogenesis by guiding the progressive worsening in grade of dysplasia. Moreover, the expression of Glucose Transporter 1 (GLUT1), which is upregulated in response to hypoxia-inducible factor (HIF) alpha [40], was significantly increased in dysplastic tissues and correlated well with the proliferation marker. In addition, in another study, Carbonic anhydrase 9 (CAIX) expression, as an endpoint of hypoxia-aerobic glycolysis-acidosis sequence, proved to be an independent risk factor of OCC malignant transformation [41].

In support of the prognostic significance of the hypoxic cluster, our stratification model demonstrated that the Cl3 subtype is independently associated with a significantly higher risk of malignant transformation. Notably, the classifier developed using a 110-gene signature reliably identified Cl3 lesions across an independent dataset, further confirming its clinical relevance. These findings strengthen the case for integrating molecular profiling into risk assessment models for OPMDs and pave the way for the development of a clinical grade assay.

In the complex framework of understanding the role of hypoxia in the malignant transformation of OPMDs, this study introduces an additional pivotal factor: the oral microbiome. The intratumoral microbiota can influence cancer progression through multiple mechanisms, such as inducing genetic mutations in the host, reshaping the immune environment, and modulating cancer metabolism along with oncogenic pathways [42]. Indeed, our series of OPMDs samples belonging to the hypoxia cluster showed a significant abundance of Fusobacterium bacterial genera, namely *Fusobacterium Nucleatum*, suggesting a substantial impact of hypoxia on the composition of the microbial community. After evaluating microbial composition, we also analyzed the activity of the bacteria through a protein transcription analysis. *Fusobacterium nucleatum* was present and active, as evidenced by the upregulation of the rpsE gene involved in protein transcription.

Khan and colleagues [43] performed a whole transcriptome of 66

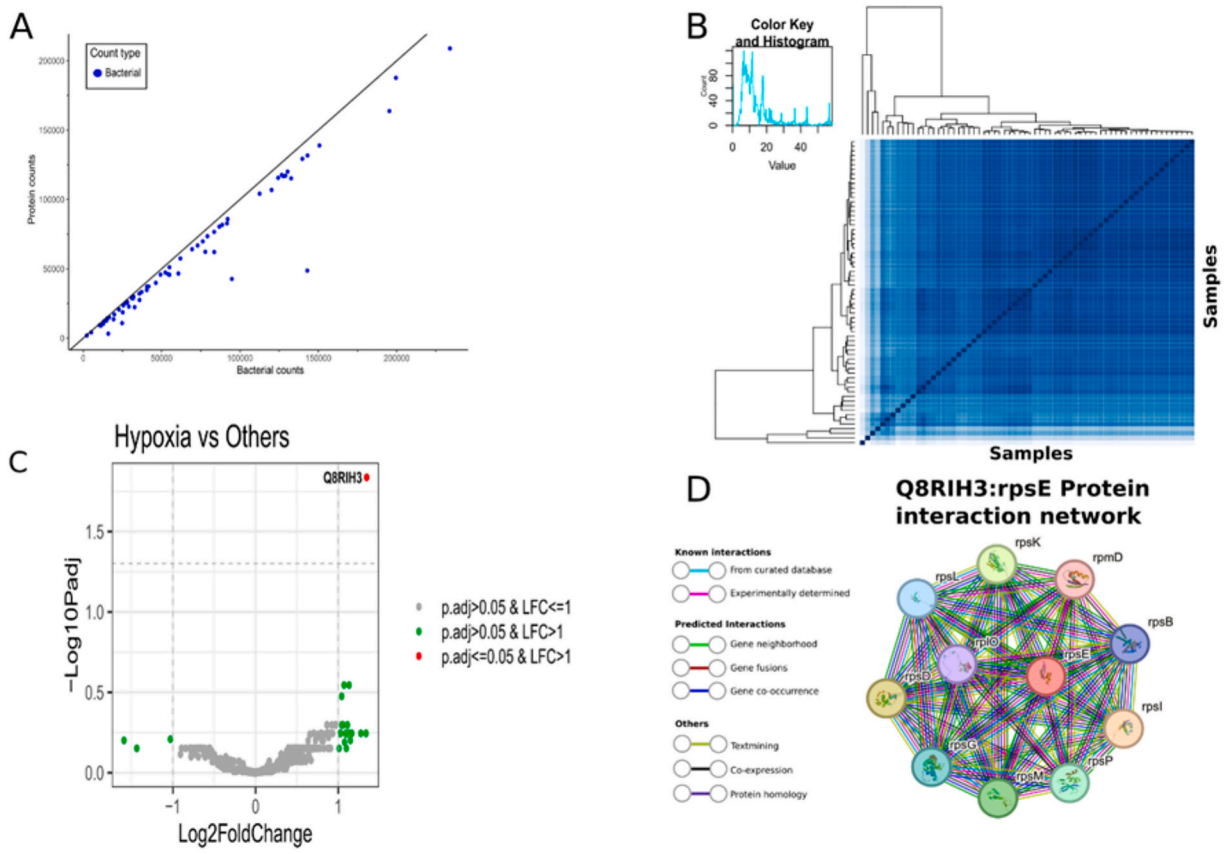

Fig. 4. Metaproteomic analysis of translated microbial sequences (A) Comparative analysis of feature counts between bacterial reads aligned to the NCBI metagenome database and the protein counts resulting from translated alignment against the Swiss-Prot database. (B) Correlation plot depicting the protein composition relationships among the samples. (C) Volcano plot illustrating differentially expressed proteins identified using the LinDA package. Notably, Q8EIH3, a ribosomal protein within *Fusobacterium nucleatum's* proteome, showed significant differential expression under hypoxic conditions (adjusted p-value < 0.05 and Log2FoldChange > 1). (D) Network representation of the interactome involving Fusobacterium nucleatum's Q8EIH3 (SSU ribosomal protein S5P), visualized using Cytoscape.

cases comprising premalignant lesions, healthy controls and oral cavity cancers (OCC). Their data showed that premalignant lesions were associated with enriched epithelial-mesenchymal transition (EMT) and immune response gene signatures. Interestingly, they did not limit their analysis to the transcriptome, but they also evaluated the relative microbial abundance in the same case series. Among the microbial genera significantly more abundant in oral cavity cancer and premalignant lesions were included Fusobacterium, Shewanella, and the fungus Candida, all recognized to be associated with OCC. Also, through their analysis they suggested a potential role of the oral microbiome in selecting molecular pathways involved in carcinogenesis.

Once again, defining whether the chicken or the egg was hatched first is complex. As a matter of fact, we cannot determine with any degree of certainty whether the hypoxic environment selects a microbiota favoring neoplastic transformation or whether the different composition of the microbiota affects gene expression by disfavoring OPMD patients' prognosis.

Probably the answer does not lie in a single mechanism, but rather is a combination of multiple co-presenting factors. Therefore, further functional studies are needed to define the causative role of microbiome on microenvironment differentiation towards pathways more prone to transform into cancer. In this regard, our observation that hypoxic cluster is linked to Fusobacterium could be a mechanistic explanation about the interlink of these two major actors in malignant transformation. The exact chain of events that links an altered microbiome with transcriptome-characterized OPMD should be studied in larger series, to better depict the carcinogenesis cascade.

Statement of ethics

This study was approved by the ethic committee of Brescia (study number NP4713).

All patients provided informed written consent for sample and data collection for the biomarker research.

Data availability

MIAME-compliant data are deposited in the GEO repository (GSE302239).

CRediT authorship contribution statement

Cristina Gurizzan: Writing – original draft, Investigation, Formal analysis. **Armando G. Licata:** Writing – original draft, Visualization, Methodology, Formal analysis. **Luigi Lorini:** Investigation, Data curation. **Cesare Piazza:** Resources. **Davide Mattavelli:** Formal analysis. **Alberto Paderno:** Resources. **Simonetta Battocchio:** Resources. **Laura Ardighieri:** Resources. **Anna Bozzola:** Resources. **Carlo Resteghini:** Resources, Investigation. **Chiara Magri:** Resources. **Chiara Romani:** Writing – review & editing, Resources. **Deborah Lenoci:** Investigation, Formal analysis. **Marta Lucchetta:** Visualization, Methodology, Formal analysis. **Mara S. Serafini:** Formal analysis. **Loris De Cecco:** Visualization, Methodology, Investigation, Funding acquisition, Formal analysis, Data curation, Conceptualization. **Paolo Bossi:** Writing – review & editing, Writing – original draft, Investigation, Funding acquisition, Data curation, Conceptualization.

Declaration of competing interest

The authors declare the following financial interests/personal relationships which may be considered as potential competing interests: PB reported the following conflict of interests in the past 3 years: Participation to advisory board or conference honoraria for Merck, Sanofi-Regeneron, Merck Sharp & Dohme, Sun Pharma, Angelini, Nestlè, Elevar. All other authors reported no conflict of interest.

Acknowledgement

This work was supported by the Associazione Italiana per la Ricerca sul Cancro (AIRC) (IG21740 to PB).

Appendix A. Supplementary data

Supplementary data to this article can be found online at https://doi.org/10.1016/j.oraloncology.2025.107583.

References

[1] Warnakulasuriya S, Johnson NW, Van Der Waal I. Nomenclature and classification of potentially malignant disorders of the oral mucosa. J Oral Pathol Med 2007;36:575–80. https://doi.org/10.1111/j.1600-0714.2007.00582.x.
[2] Kerr AR, Lodi G. Management of oral potentially malignant disorders. Oral Dis 2021;27:2008–25. https://doi.org/10.1111/odi.13980.
[3] Mello FW, Miguel AFP, Dutra KL, Porporatti AL, Warnakulasuriya S, Guerra ENS, et al. Prevalence of oral potentially malignant disorders: a systematic review and meta-analysis. J Oral Pathol Med 2018;47:633–40. https://doi.org/10.1111/jop.12726.
[4] Oliveira MB dos R, Mello FC de Q, Paschoal MEM. The relationship between lung cancer histology and the clinicopathological characteristics of bone metastases. Lung Cancer 2016. https://doi.org/10.1016/j.lungcan.2016.03.014.
[5] Cai X, Zhang J, Han Y, Tang Q, Zhang H, Li T. Development and validation of a nomogram prediction model for malignant transformation of oral potentially malignant disorders. Oral Oncol 2021;123:105619. https://doi.org/10.1016/j.oraloncology.2021.105619.
[6] Chiu S-F, Ho C-H, Chen Y-C, Wu L-W, Chen Y-L, Wu J-H, et al. Malignant transformation of oral potentially malignant disorders in Taiwan. Medicine 2021;100:e24934. https://doi.org/10.1097/MD.0000000000024934.
[7] Gurizzan C, Lorini L, Bossi P. Oral potentially malignant disorders: new insights for future treatment. Curr Opin Otolaryngol Head Neck Surg 2021;29:138–42. https://doi.org/10.1097/MOO.0000000000000695.
[8] Iocca O, Sollecito TP, Alawi F, Weinstein GS, Newman JG, De Virgilio A, et al. Potentially malignant disorders of the oral cavity and oral dysplasia: a systematic review and meta-analysis of malignant transformation rate by subtype. Head Neck 2020;42:539–55. https://doi.org/10.1002/hed.26006.
[9] Mao L, Lee JS, Fan YH, Ro JY, Batsakis JG, Lippman S, et al. Frequent microsatellite alterations at chromosomes 9p21 and 3p14 in oral premalignant lesions and their value in cancer risk assessment. Nat Med 1996;2:682–5. https://doi.org/10.1038/nm0696-682.
[10] Lee JJ, Hong WK, Hittelman WN, Mao L, Lotan R, Shin DM, et al. Predicting cancer development in oral leukoplakia: ten years of translational research. Clin Cancer Res 2000.
[11] William WN, Lee W-C, Lee JJ, Lin HY, Eterovic AK, El-Naggar AK, et al. Genomic and transcriptomic landscape of oral pre-cancers (OPCs) and risk of oral cancer (OC). J Clin Oncol 2019;37:6009. https://doi.org/10.1200/JCO.2019.37.15_suppl.6009.
[12] Carenzo A, Serafini MS, Roca E, Paderno A, Mattavelli D, Romani C, et al. Gene expression clustering and selected head and neck cancer gene signatures highlight risk probability differences in oral premalignant lesions. Cells 9 2020. https://doi.org/10.3390/cells9081828.
[13] Liu N-N, Jiao N, Tan J-C, Wang Z, Wu D, Wang A-J, et al. Multi-kingdom microbiota analyses identify bacterial–fungal interactions and biomarkers of colorectal cancer across cohorts. Nat Microbiol 2022;7:238–50. https://doi.org/10.1038/s41564-021-01030-7.
[14] Le Noci V, Guglielmetti S, Arioli S, Camisaschi C, Bianchi F, Sommariva M, et al. Modulation of pulmonary microbiota by antibiotic or probiotic aerosol therapy: a strategy to promote immunosurveillance against lung metastases. Cell Rep 2018;24:3528–38. https://doi.org/10.1016/j.celrep.2018.08.090.
[15] Nejman D, Livyatan I, Fuks G, Gavert N, Zwang Y, Geller LT, et al. The human tumor microbiome is composed of tumor type–specific intracellular bacteria. Science 1979;368(2020):973–80. https://doi.org/10.1126/science.aay9189.
[16] Sepich-Poore GD, Zitvogel L, Straussman R, Hasty J, Wargo JA, Knight R. The microbiome and human cancer. Science (1979) 2021;371. https://doi.org/10.1126/science.abc4552.
[17] Hanahan D. Hallmarks of cancer: new dimensions. Cancer Discov 2022;12:31–46. https://doi.org/10.1158/2159-8290.CD-21-1059.
[18] de Cecco L, Nicolau M, Giannoccaro M, Daidone MG, Bossi P, Locati L, et al. Head and neck cancer subtypes with biological and clinical relevance: Meta-analysis of gene-expression data. Oncotarget 2015. https://doi.org/10.18632/oncotarget.3301.
[19] Tibshirani R, Hastie T, Narasimhan B, Chu G. Diagnosis of multiple cancer types by shrunken centroids of gene expression. Proc Natl Acad Sci 2002;99:6567–72. https://doi.org/10.1073/pnas.082099299.
[20] Jing S-L, Afshari K, Guo Z-C. Inflammatory response-related genes predict prognosis in patients with HNSCC. Immunol Lett 2023;259:46–60. https://doi.org/10.1016/j.imlet.2023.06.003.
[21] Han Y, Ding Z, Chen B, Liu Y, Liu Y. A novel inflammatory response–related gene signature improves high-risk survival prediction in patients with head and neck squamous cell carcinoma. Front Genet 2022;13:767166. https://doi.org/10.3389/fgene.2022.767166.
[22] Carenzo A, Pistore F, Serafini MS, Lenoci D, Licata AG, De Cecco L. hacksig: a unified and tidy R framework to easily compute gene expression signature scores. Bioinformatics 2022;38:2940–2. https://doi.org/10.1093/bioinformatics/btac161.
[23] Robin X, Turck N, Hainard A, Tiberti N, Lisacek F, Sanchez J-C, et al. pROC: an open-source package for R and S+ to analyze and compare ROC curves. BMC Bioinf 2011;12:77. https://doi.org/10.1186/1471-2105-12-77.
[24] Wickham H, Averick M, Bryan J, Chang W, McGowan L, François R, et al. Welcome to the tidyverse. J Open Source Softw 2019;4:1686. https://doi.org/10.21105/joss.01686.
[25] McMurdie PJ, Holmes S. phyloseq: an R package for reproducible interactive analysis and graphics of microbiome census data. PLoS One 2013;8:e61217. https://doi.org/10.1371/journal.pone.0061217.
[26] Love MI, Huber W, Anders S. Moderated estimation of fold change and dispersion for RNA-seq data with DESeq2. Genome Biol 2014;15:550. https://doi.org/10.1186/s13059-014-0550-8.
[27] Buchfink B, Reuter K, Drost H-G. Sensitive protein alignments at tree-of-life scale using DIAMOND. Nat Methods 2021;18:366–8. https://doi.org/10.1038/s41592-021-01101-x.
[28] Zhou H, He K, Chen J, Zhang X. LinDA: linear models for differential abundance analysis of microbiome compositional data. Genome Biol 2022;23:95. https://doi.org/10.1186/s13059-022-02655-5.
[29] Shannon P, Markiel A, Ozier O, Baliga NS, Wang JT, Ramage D, et al. Cytoscape: a software environment for integrated models of biomolecular interaction networks. Genome Res 2003;13:2498–504. https://doi.org/10.1101/gr.1239303.
[30] William WN, Papadimitrakopoulou V, Lee JJ, Mao L, Cohen EEW, Lin HY, et al. Erlotinib and the risk of oral cancer: the erlotinib prevention of oral cancer (EPOC) randomized clinical trial. JAMA Oncol 2016;2:209–16. https://doi.org/10.1001/jamaoncol.2015.4364.
[31] Foy J-P, Bertolus C, Ortiz-Cuaran S, Albaret M-A, Williams WN, Lang W, et al. Immunological and classical subtypes of oral premalignant lesions. Oncoimmunology 2018;7:e1496880. https://doi.org/10.1080/2162402X.2018.1496880.
[32] Hanna GJ, Villa A, Mistry N, Jia Y, Quinn CT, Turner MM, et al. Comprehensive immunoprofiling of high-risk oral proliferative and localized leukoplakia. Cancer Res Commun 2021;1:30–40. https://doi.org/10.1158/2767-9764.CRC-21-0060.
[33] Nicolau M, Tibshirani R, Børresen-Dale A-L, Jeffrey SS. Disease-specific genomic analysis: identifying the signature of pathologic biology. Bioinformatics 2007;23:957–65. https://doi.org/10.1093/bioinformatics/btm033.
[34] Serafini MS, Cavalieri S, Licitra L, Pistore F, Lenoci D, Canevari S, et al. De Cecco, Association of a gene-expression subtype to outcome and treatment response in patients with recurrent/metastatic head and neck squamous cell carcinoma treated with nivolumab. J Immunother Cancer 2024;12:e007823. https://doi.org/10.1136/jitc-2023-007823.
[35] Machiels J-P, Bossi P, Menis J, Lia M, Fortpied C, Liu Y, et al. Activity and safety of afatinib in a window preoperative EORTC study in patients with squamous cell carcinoma of the head and neck (SCCHN). Ann Oncol 2018;29:985–91. https://doi.org/10.1093/annonc/mdy013.
[36] Bossi P, Bergamini C, Siano M, Cossu Rocca M, Sponghini AP, Favales F, et al. De Cecco, functional genomics uncover the biology behind the responsiveness of head and neck squamous cell cancer patients to cetuximab. Clin Cancer Res 2016;22:3961–70. https://doi.org/10.1158/1078-0432.CCR-15-2547.
[37] Lenoci D, Carenzo A, Cavalieri S, Pistore F, Serafini MS, Bossi P, et al. Biological properties of hypoxia-related gene expression models/signatures on clinical benefit of anti-EGFR treatment in two head and neck cancer window-of-opportunity trials. Oral Oncol 2022;126:105756. https://doi.org/10.1016/j.oraloncology.2022.105756.
[38] Tonella L, Giannoccaro M, Alfieri S, Canevari S, De Cecco L. Gene expression signatures for head and neck cancer patient stratification: are results ready for clinical application? Curr Treat Options Oncol 2017;18:32. https://doi.org/10.1007/s11864-017-0472-2.
[39] Kujan O, Shearston K, Farah CS. The role of hypoxia in oral cancer and potentially malignant disorders: a review. J Oral Pathol Med 2017;46:246–52. https://doi.org/10.1111/jop.12488.
[40] Grimm M, Cetindis M, Lehmann M, Biegner T, Munz A, Teriete P, et al. Association of cancer metabolism-related proteins with oral carcinogenesis – indications for chemoprevention and metabolic sensitizing of oral squamous cell carcinoma? J Transl Med 2014;12:208. https://doi.org/10.1186/1479-5876-12-208.
[41] Zhang X, Han S, Han H-Y, Heon Ryu M, Kim K-Y, Choi E-J, et al. Risk prediction for malignant conversion of oral epithelial dysplasia by hypoxia related protein

expression. Pathology 2013;45:478–83. https://doi.org/10.1097/PAT.0b013e3283632624.
[42] Huang J, Mao Y, Wang L. The crosstalk of intratumor bacteria and the tumor. Front Cell Infect Microbiol 2024;13:1273254. https://doi.org/10.3389/fcimb.2023.1273254.
[43] Khan MM, Frustino J, Villa A, Nguyen B-C, Woo S-B, Johnson WE, et al. Total RNA sequencing reveals gene expression and microbial alterations shared by oral pre-malignant lesions and cancer. Hum Genomics 2023;17:72. https://doi.org/10.1186/s40246-023-00519-y.